A high-temperature stable spectrally-selective solar absorber based on cermet of titanium nitride in SiO2 deposited on lanthanum…

Article *in* Solar Energy Materials and Solar Cells · February 2017

DOI: 10.1016/j.solmat.2016.10.012

6 authors, including:

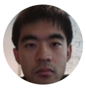

Lu Tang
University of Houston

Alexander P. Litvinchuk
University of Houston

Jiming Bao
University of Houston

Zhifeng Ren
Boston College, USA

Solar Energy Materials & Solar Cells 160 (2017) 12–17

Contents lists available at ScienceDirect

Solar Energy Materials & Solar Cells

journal homepage: www.elsevier.com/locate/solmat

A high-temperature stable spectrally-selective solar absorber based on cermet of titanium nitride in SiO_2 deposited on lanthanum aluminate

Feng Cao[a,b], Lu Tang[b], Yang Li[c], Alexander P. Litvinchuk[b], Jiming Bao[c], Zhifeng Ren[b,*]

[a] School of Science, Harbin Institute of Technology, Shenzhen, Guangdong 518055, China
[b] Department of Physics and TcSUH, University of Houston, Houston, TX 77204, USA
[c] Department of Electrical and Computer Engineering, University of Houston, Houston, TX 77204, USA

A R T I C L E I N F O

Keywords:
Solar absorber
Cermet
Solar absorptance
Thermal emittance
Spectral selectivity

A B S T R A C T

Spectrally-selective solar absorber is required to be thermally stable at high operational temperature. However the currently available absorbers aren't stable beyond 700 °C. Here we explore a new absorber with cermet of TiN in SiO_2 on $LaAlO_3$ substrate that can be used for long term at 700 °C. The optimized cermets contain TiN with volume fraction of 60% and 65% as sun-light absorption media, SiO_2 as anti-reflection coating (ARC), and tungsten (W) as infrared (IR) reflection layer. The absorbers demonstrate an absorptance higher than ~95% before annealing and ~94% after annealing at 700 °C, which will be useful for especially concentrated solar applications.

1. Introduction

Solar thermal technologies converting the abundant solar energy into heat and then to electricity have attracted extensive attention in recent years. In the solar thermal process, the absorbed heat can be directly utilized for domestic hot water, or further converted into electricity via steam turbines [1], solar thermoelectric generators [2], solar thermophotovoltaic [3,4], and solar thermionic generators [5]. Concentrating solar power (CSP) has an increased deployment all over the world [6,7]. The solar thermal system conversion efficiency in CSP can be separated into the sunlight-to-thermal efficiency and thermal-to-electricity efficiency. The sunlight-to-thermal efficiency is strongly relied on the optical properties of solar absorbers. The ideal spectrally-selective solar absorber should have a near-blackbody absorptance (α) in a certain wavelength region while suppressing the emission in IR range at operational temperatures [7]. The thermal-to-electricity conversion efficiency is capped by Carnot efficiency, $\eta_c=1-T_c/T_h$, where T_h is working temperature, and T_c is the ambient temperature. The efficiency can be boosted by increasing the working temperature, which requires stable solar absorber at elevated temperatures.

How to further enhance the stable temperature of selective surfaces beyond 700 °C is still a challenge. A variety of spectrally-selective solar absorbers such as intrinsic absorbers, cermet-based absorbers and metallic nanostructure-enabled absorbers have been extensively explored for potential applications at high temperatures. The intrinsic absorbers, such as $Si_{0.8}Ge_{0.2}$, demonstrated an absorptance of ~0.90–0.95 and a relatively low infrared (IR) emissivity of less than 0.3 at 500 °C.[8] Cermet-based absorbers have indicated good performances on the spectral selectivity and thermal stability [9–11]. The high solar absorptance is due to the interband transitions in the metal and small particle plasmonic resonances, and the good thermal stability is ensured by the stable ceramic host. The tandem absorber of TiAlN/TiAlON/Si_3N_4 exhibited a high solar absorptance of 0.95, a low emittance of 0.07 at 82 °C, as well as thermal stability in air up to 600 °C for 2 h [12]. The Mo-Si_3N_4 based selective coatings demonstrated a high solar absorptance of 0.93 and low emittance of 0.11 at 600 °C estimated from a single-angle bidirectional reflectance spectrum. However the coatings showed unsatisfactory thermal stability because the emittance at 600 °C increased to 0.15 after thermal cycling at 600 °C for 15 h with the heating rate of 4 °C/min [13]. The tungsten (W) and nickel (Ni) filled Al_2O_3 and YSZ cermet based spectrally-selective solar absorbers indicated better thermal stability at 600 °C for seven days in vacuum and high solar absorptance of 0.90–0.91, as well as low total hemispherical emittance of 0.13–0.15 at 500 °C.[14,15] The Ni nanopyramids based solar absorbers also demonstrated high thermal stability after a heat treatment at 800 °C in vacuum for 5 h with absorptance of 0.9 and emittance of 0.09 at 400 °C calculated from the absorptance spectra [16]. To achieve reliable spectrally-selective solar absorbers with super thermal stability at high temperature for a long term, one route is to modify the substrates through forming a spontaneous oxide layer on stainless steel, depositing a barrier layer, or choosing nonmetallic substrates (quartz, silicon) to

* Corresponding author.
E-mail address: zren@uh.edu (Z. Ren).

http://dx.doi.org/10.1016/j.solmat.2016.10.012
Received 14 June 2016; Received in revised form 30 September 2016; Accepted 5 October 2016
0927-0248/

eliminate the effect of substrate element diffusion; another strategy is to introduce more stable metal components in the coatings, such as the noble metal Pt embedded in the Al_2O_3 matrix, which would ensure better thermal stability due to the super antioxidation resistance of the noble metal [17,18]. However the use of noble metal is not economically viable for large-scale deployment. Titanium nitride with unusual properties, such as high-temperature stability, extreme hardness, chemical inertness and metallic electrical conductivity, can be chosen as an alternative to noble metal in cermet due to its similar metallic behaviors [19,20].

In this paper, we present a reliable high-temperature spectrally-selective solar absorber with TiN-SiO_2 cermet as sun-light absorbing coating and systematically investigate the optical properties of the cermets with different TiN volume fractions. We compare the effect of different substrates including mechanically polished stainless steel (SS), SS coated with SiO_2 layer, annealed SS and LAO substrates on the spectral selectivity and thermal stability, and analyze the intrinsic change of absorbers deposited on those substrates upon annealing at different temperatures.

2. Experimental details

2.1. Preparation of coatings

All coatings are deposited by a commercial magnetron sputtering system (AJA International, Inc.) according to our previously reported method [14]. Briefly, the metals and dielectric materials are deposited by a DC and a RF magnetron sputtering, respectively, and the cermet layers are deposited by co-sputtering of the conductive ceramic and the dielectric materials. The multilayer stack includes, starting from the substrate, one W IR-reflecting layer, two TiN-SiO_2 cermet layers (C4 and C5) with high and low metal volume fractions in SiO_2 ceramic host, and one SiO_2 anti-reflection coating (ARC) layer (Fig. 1). The targets are high purity tungsten (99.95%, 2″ Dia.), TiN (99.5%, 3″ Dia), and SiO_2 (99.995%, 3″ Dia.). Prior to the deposition process, the SS substrates are coated with 100 nm SiO_2 by RF sputtering of SiO_2 (denoted as SiO_2-SS), or with Fe_2O_3 layers by annealing the SS at 500 °C for 1 h (denoted as Ann-SS).

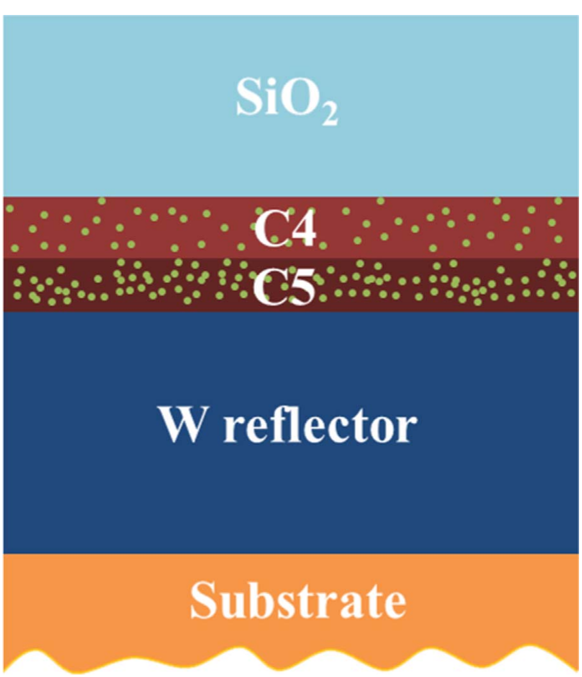

Fig. 1. Schematic of the cermet-based spectrally-selective solar absorber comprising two cermet layers C4 and C5 with different TiN volume fractions, one SiO_2 ARC layer, and one tungsten IR reflecting layer on a variety of substrates (SS, Ann-SS, SiO_2-SS, and LAO).

2.2. Material characterizations and optical measurements

The phases of samples are characterized using a T64000 Raman spectrometer (Horiba Jobin Yvon) in back-scattering geometry at room temperature with an air cooled Ar-ion laser (514 nm) as the excitation source. The morphology and roughness of the surfaces are measured with a Veeco Dimension 3000 Atomic Force Microscope (AFM). The thicknesses of the prepared coatings are measured with an Alpha-step 200 Profilometer (Tencor). The spectral directional-hemispherical reflectance from 0.3 to 2.5 µm is measured with a Cary 5000 UV–Vis–NIR spectrophotometer equipped with a diffuse reflectance accessory (DRA) at an incident angle of 3° 20′. The specular bi-directional reflectance in the wavelength range of 2.5–25 µm is recorded on a Nicolet iS50 FT-IR spectrometer with a gold mirror (Thorlabs) as reference at an incident angle of 10°. Optical properties of cermets with different TiN volume fractions are obtained using a variable-angle M-2000 spectroscopic ellipsometer (J. A. Woollam Co.). The thermal stability is carried out in a tubular furnace at temperatures of 600 °C, 650 °C, and 700 °C for 7 days under a vacuum pressure of ~5×10^{-3} Torr.

3. Results and discussion

The fabricated spectrally selective solar absorbers for high-temperature applications are based on a double-cermet configuration with one SiO_2 ARC layer and a metal tungsten layer with high IR reflectance as diffusion barrier (Fig. 1). In order to investigate the effect of substrates on thermal stability and spectral selectivity, the solar absorbers are deposited on a variety of substrates (SS, Ann-SS, SiO_2-SS, and LAO). The detailed parameters are summarized in Table 1.

The stainless steel (SS) has been extensively investigated as the substrate of higher temperature spectrally-selective solar absorber due to its higher thermal stability and cost-effectiveness compared with copper or aluminum substrate utilized in commercialized solar absorber for applications below 500 °C. However the stability of absorber deposited on the SS substrate is undermined by the oxidation or diffusion of stainless steel as the temperature is higher than 650 °C [21]. To suppress the effect of the substrate element diffusion on the performance, modification of the substrate is carried out on mechanically polished SS substrate. The AFM images of the pristine SS, annealed SS (Ann-SS, annealed at 500 °C for 1 h) and SiO_2-coated SS (SiO_2-SS) are shown in Fig. 2. The SS and SiO_2-SS have a smooth surface with a root mean square roughness (R_q) of 1.5 nm and 2.1 nm, respectively. The Ann-SS has a rough surface (Fig. 2b) with R_q of 16.8 nm and particle size of 200–300 nm due to the simultaneously formed rough oxides layer upon annealing in air. The optical responses of those substrates (Fig. 2d) show huge difference on the reflectance curve, especially in the wavelength range of below 4 µm, and less discrepancy in the mid-IR range. The pristine SS displays a high

Table 1
Sputtering parameters of the optimized spectrally-selective solar absorbers on various substrates.

Sample	Substrate	W IR reflector	C5	C4	SiO_2 ARC
TSS_SS	SS	150 nm	33 nm	38 nm	114 nm
TSS_Ann-SS	Ann-SS	150 nm	33 nm	38 nm	114 nm
TSS_SS-SiO_2	SiO_2-SS	150 nm	33 nm	38 nm	114 nm
TSS_LAO	LAO	150 nm	33 nm	38 nm	114 nm

Tungsten IR reflecting layer: sputtered at a DC power density of 2.2 W/cm^2.
Cermet (C4 and C5): TiN-SiO_2 sputtered using two individual RF power supplies with different TiN volume fractions in cermet. The TiN volume fraction of cermet is 60% and 65% for C4 and C5, respectively.
ARC:SiO_2 sputtered with a RF power density of 4.4 W/cm^2.

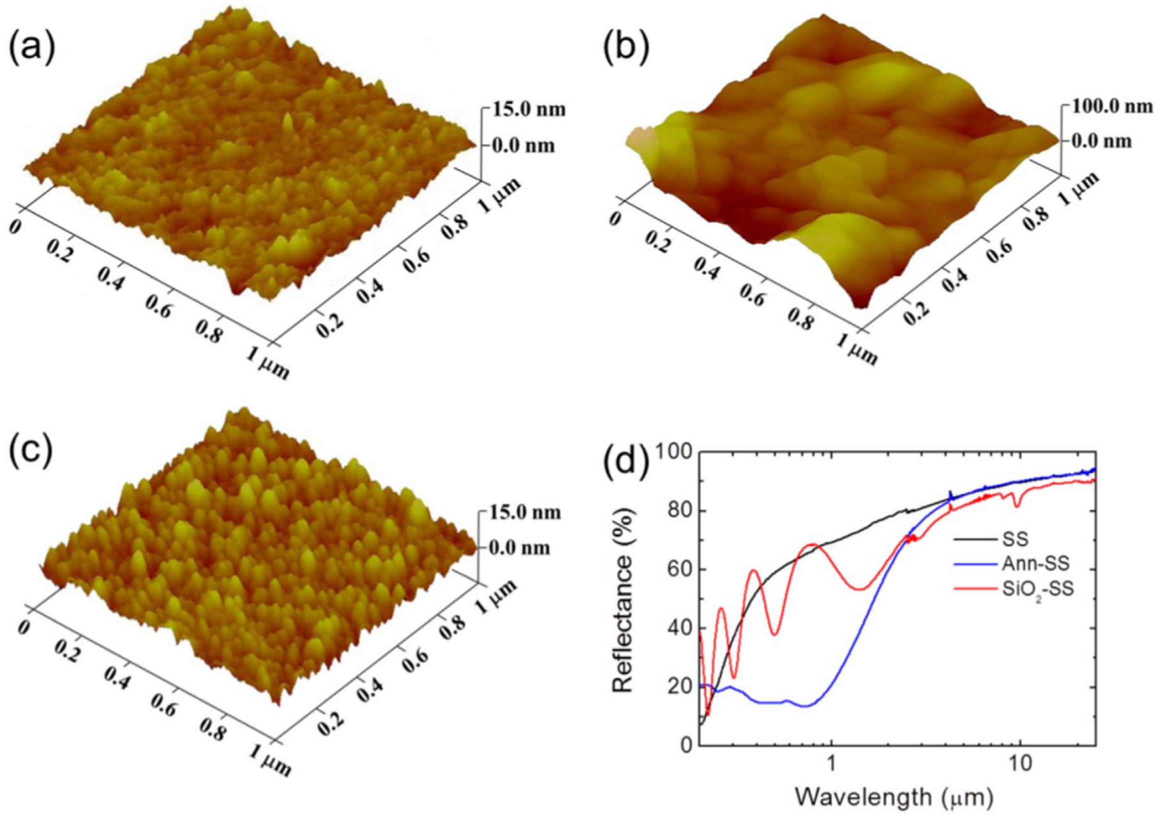

Fig. 2. AFM images of the pristine SS (a), Annealed SS (b) and SiO_2-SS with 100 nm SiO_2 (c). (d) the reflectance spectra of the pristine SS (black line), Ann-SS (blue line) and SiO_2-SS (red line). (For interpretation of the references to color in this figure legend, the reader is referred to the web version of this article.).

reflectance in this regime (below 4 μm) indicting metallic characteristics. There are many interference peaks on SiO_2-SS due to the oxide layer. The low reflectance in the Ann-SS suggests a high absorptance since the substrate is opaque, which is resulted from the formed rough oxides layer on SS. The absorbers would have similar morphology to their corresponding substrates, so the substrate morphology has a significant contribution to the spectral selectivity and thermal stability.

The cermet in cermet-based spectrally-selective solar absorbers plays a crucial role in sunlight absorbing [11]. The optical constants of cermet, especially the extinction coefficient, have a direct contribution to the absorption. To tune the optical characteristics of TiN-SiO_2 cermet, cermets with different TiN volume fractions from 29–65% in SiO_2 host are deposited on Si substrates. The Kramers-Kronig consistent B-spline model [22,23] is used to extract the n and k of cermets in CompleteEASE software (J. A. Woollam Co.) as shown in Fig. 3. Cermets with low TiN volume fractions (C1 and C2) depict a transparent dielectric-like characteristic with the extinction coefficient of zero below the bandgap. The refractive index increases with increasing the TiN volume fractions from 29% (C1) to 41% (C2). So the optical characteristics of cermets with lower than 41% TiN volume fraction are dominated by the SiO_2 host. The cermets C3, C4, and C5 with increasing the TiN volume fraction in SiO_2 have a nonzero k value over the wavelength range of 500–1690 nm, indicating a boosted absorption of solar radiation mainly caused by the interband transitions in TiN and small particle plasmonic resonances [7]. It looks like the k value has not reached the maximum, which means the absorption performance of cermet can be further promoted by incorporating more TiN component in cermet. However, more TiN amount in cermet would undermine thermal stability due to lack of effective protection from the stable SiO_2 host. So in the following section we mainly focus on C4 and C5 to optimize the performances.

Fig. 4 shows the optical responses of optimized spectrally-selective solar absorber (TSS) with C4 and C5 cermets deposited on SS, Ann-SS

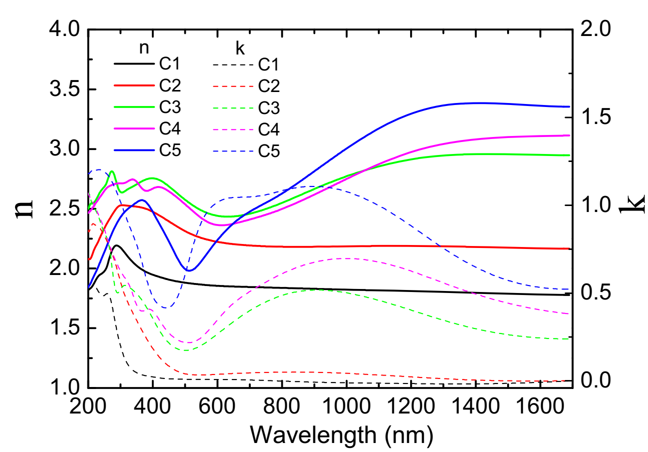

Fig. 3. The refractive index (n) and extinction coefficient (k) of cermets with different TiN volume fractions in SiO_2 host. The TiN volume fractions in C1, C2, C3, C4, and C5 are 29%, 41%, 54%, 60%, and 65%, respectively.

and SiO_2-SS substrates. The minor discrepancy on the reflectance spectra in the wavelength below 0.7 μm appears between the TSS_SS and TSS_Ann-SS, whereas they are almost identical between TSS_SS and TSS_SiO_2-SS. The absorber of TSS_Ann-SS demonstrates a low reflectance resulting from the rough and high absorption substrate, which enables a high solar absorptance. Furthermore, a high reflection peak located in the wavelength rang of 400–500 nm on all those absorbers is probably linked to the interference among cermet layers and the dip of k of C4 and C5 in this range depicted in Fig. 3. In order to promote the solar absorptance, the transition wavelength is shifted to longer wavelength (~1.6 μm) compared with our previous design (~1.3 μm) [15]. Consequently, the solar absorptance is enhanced from ~92% to ~95%. The thermal emittance inevitably increases due to the

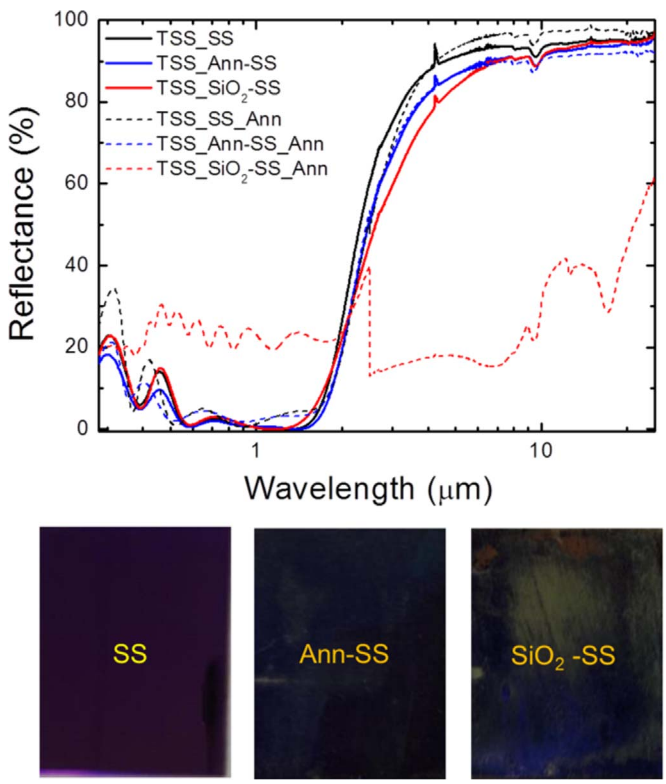

Fig. 4. The reflectance spectra of TSS with C4 and C5 double cermet structure deposited on SS (TSS_SS, black line), the annealed SS (TSS_Ann-SS, blue line) and SiO_2-SS (TSS_SiO_2-SS, red line) before (solid line) and after (dash line) annealing at 600 °C for 7 days, optical images of those absorbers after annealing (bottom) are also shown. (For interpretation of the references to color in this figure legend, the reader is referred to the web version of this article.).

redshift of spectrum, which can be compensated through increasing the optical concentration and then decreasing the weighting factor as taking into account the eventual conversion efficiency. In the mid-IR range, the absorber of TSS_SS indicates a sharp transition from low reflectance to high reflectance compared with TSS_Ann-SS and TSS_SiO_2-SS suggesting the W IR reflector deposited on mechanically polished SS substrate is favorable for IR reflection. After annealing at 600 °C for 7 days in vacuum, there is a slight change on the reflectance spectra of TSS_SS and TSS_Ann-SS, while huge degradation appears in TSS_SiO_2-SS. The coatings deposited on SS and Ann-SS have a pretty strong bonding even upon annealing, nevertheless, the coating deposited on TSS_SiO_2-SS exhibits a weak mechanical property after annealing as shown at the bottom of Fig. 4 resulting in the unfavorable change on the reflectance spectrum, which can be ascribed to the stress induced by the annealing process as a result of the different thermal expansion coefficients between the coating and its substrate [24]. Since the coating on the SiO_2 coated SS substrate cannot survive the annealing at 600 °C, it is screened in the following more rigorous evaluation.

To find out the highest operational temperature, we evaluated the thermal reliability of the absorbers deposited on SS and annealed SS substrates by annealing the absorbers at 650 °C and 700 °C. Fig. 5a shows the optical responses of those absorbers before and after annealing at 650 °C. The reflectance of both absorbers in the wavelength of below 2 μm increases slightly as a result of the possible change of optical constants in the cermet layers after annealing. The solar absorptance drops ~3% for TSS_SS (from ~95.0% to ~92.4%) and ~4% for TSS_Ann-SS (from ~96.2% to ~92.1%) as shown in Table 2. Both TSS_SS and TSS_Ann-SS absorbers demonstrate a similar solar absorptance (~92%) after annealing at 650 °C. Accordingly, the negligible advantage on the solar absorptance caused

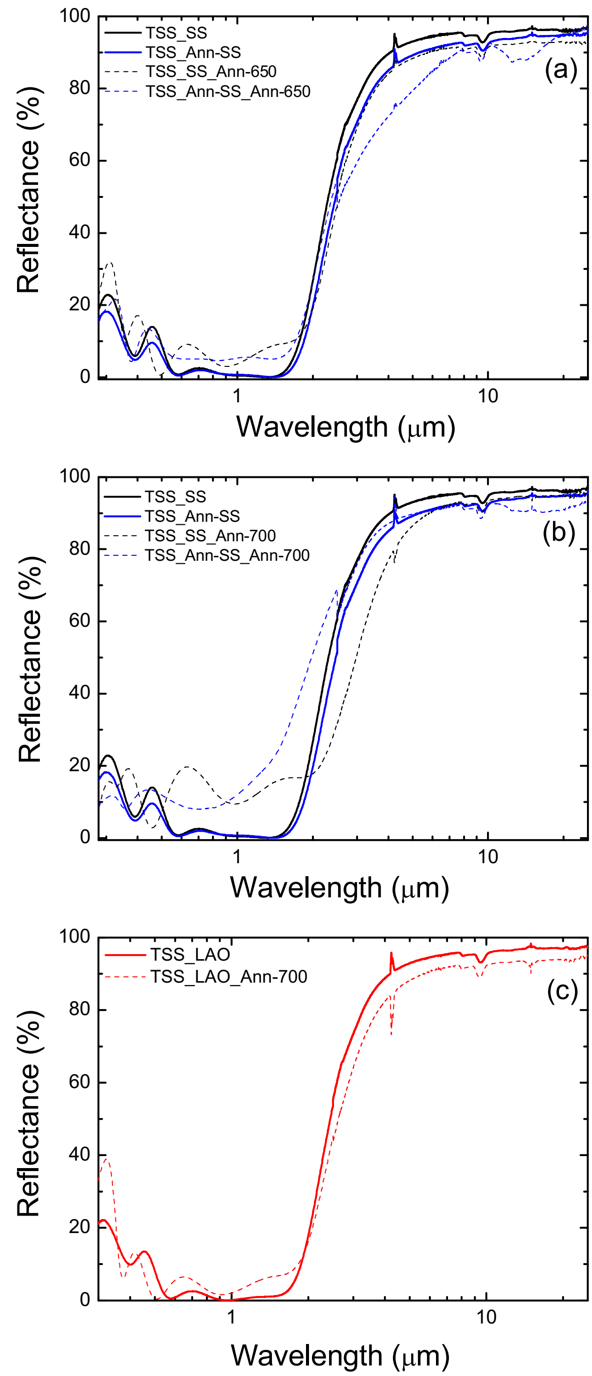

Fig. 5. The reflectance spectra of TSS with C4 and C5 double cermet structure deposited on SS (TSS_SS, black line) and annealed SS (TSS_Ann-SS, blue line) before (solid line) and after (dash line) annealing in vacuum for 7 days at 650 °C (a) and 700 °C (b). (c) The optical response of TSS_LAO before (red solid line) and after (red dash line) annealing at 700 °C. (For interpretation of the references to color in this figure legend, the reader is referred to the web version of this article.).

by the annealed substrate (Fig. 5b) cannot be preserved upon annealing at 650 °C. TSS_Ann-SS, meanwhile, shows the unfavorable thermal re-radiation characteristics owing to the higher emittance estimated from the reflectance spectrum and the blackbody radiation spectrum at 82 °C (Table 2) compared with TSS_SS absorber. Even though the formed oxides diffusion layer on the stainless steel substrate through annealing in air facilitated the thermal stability of Mo-Al_2O_3 cermet based solar absorber at 500 °C for a short term,[25] it is not commonly used in our system with a W barrier and IR reflecting layer. The spectrally-selective solar absorber with the unique configuration on the

Table 2
The solar absorptance and thermal emittance of the spectrally-selective solar absorbers before and after annealing at different temperatures, estimated by the weighted integration of the reflectance spectra with the solar spectrum (AM 1.5 direct+circumsolar) or the blackbody radiation spectrum (at 82 °C).

Sample	TSS_SS		TSS_Ann-SS		TSS_LAO	
	Absorptance	Emittance	Absorptance	Emittance	Absorptance	Emittance
Pristine	95.0%	4.8%	96.2%	7.1%	95.4%	4.3%
Ann−600	94.6%	3.6%	94.9%	9.8%	NA	NA
Ann−650	92.4%	8.6%	92.1%	10.8%	NA	NA
Ann−700	86.2%	7.3%	85.6%	9.0%	94.2%	8.0%

mechanically polished SS substrate demonstrates favorable reliability at 650 °C for a long term. However, both TSS_SS and TSS_Ann-SS absorbers cannot survive annealing temperature of 700 °C. The huge degradation in the solar spectra range results in lower solar absorptance (~85%) due to possibly oxidation of TiN in cermet layer at 700 °C. Furthermore, the stress between the coating and the substrate at this temperature also promote the defect formation and diffusion process within the layers contributed to the rough surface. The changes of spectral selectivity are consistent with the morphology changes of those absorbers (SI, Fig. S1 and Fig. S2) showing a big change on R_q of the absorbers annealed at 700 °C (SI, Tab. S1).

However, the degradation after annealing at 700 °C is small for absorbers deposited on LAO, as shown in Fig. 5c. The reflectance of TSS_LAO in solar spectra regime experiences a negligible change upon annealing indicating a stable solar absorptance, even though the reflectance in mid-IR range decreases leading to increase of radiation. The solar absorptance still maintains a value of higher than ~94% after annealing at 700 °C (Table 2). The cause of stable absorptance is mainly due to the stability of absorber and substrate.

To find out the mechanism of the performance degradation after annealing, we employed the Raman technique to investigate the phase change of those absorbers before and after annealing, shown in Fig. 6. There are two broad bands located in the ranges of 200–400 cm^{-1} and 500–700 cm^{-1} on the pristine samples, ascribed to the vibration of Ti atoms surrounding the nitrogen vacancy (longitudinal acoustic (LA) mode) and the vibration of N atoms surrounding the Ti vacancy (longitudinal optical (LO) mode), respectively.[26,27] After annealing at 600 °C and 650 °C, those broad peaks tend to be sharper indicating a better crystallization of TiN. For the coating on the mechanically polished stainless steel substrate (TSS_SS), the LO mode disappears as the annealing temperature increases to 700 °C suggesting the formation of more nitrogen vacancy, which would lead to the prominent morphology change (SI, Fig. S1), and the performance degradation (Fig. 5a). The coating on the annealed SS (TSS_Ann-SS, Fig. 6b) shows three distinct Raman peaks including two peaks located at ~616 cm^{-1} and ~445 cm^{-1}, which can be assigned as A_{1g} and E_g modes from rutile phase of TiO_2, respectively,[28,29] and one peak (~690 cm^{-1}) originated from the A_{1g} mode of $FeCr_2O_4$.[30] It can be concluded that the TiN component in the cermet experiences decomposition and then oxidization at annealing of 700 °C. The rough and non-dense structure of the TSS_Ann-SS absorber due to the pre-annealing process applied on the substrate would promote the oxygen diffusion in cermet layers and eventually contributes to the TiO_2 formation when it was annealed at 700 °C. As expected the Raman peaks of TiN in the coatings on LAO substrate (TSS_LAO) remain even upon annealing at 700 °C (Fig. 6c) indicating the cermets in this configuration are stable at 700 °C. It is therefore clear that the substrate has a significant effect on the change of morphology and phases of the coatings at elevated temperatures. The results obtained from Raman spectra are consistent with the optical responses (Fig. 5).

4. Conclusions

We developed stable cermets of conductive ceramics TiN in SiO_2 and systematically investigated the optical properties of the cermets with different TiN volume fractions. The cermets with the TiN volume fractions of > 54% possess the characteristics of sunlight absorption. The spectrally-selective solar absorbers with proposed cermets depos-

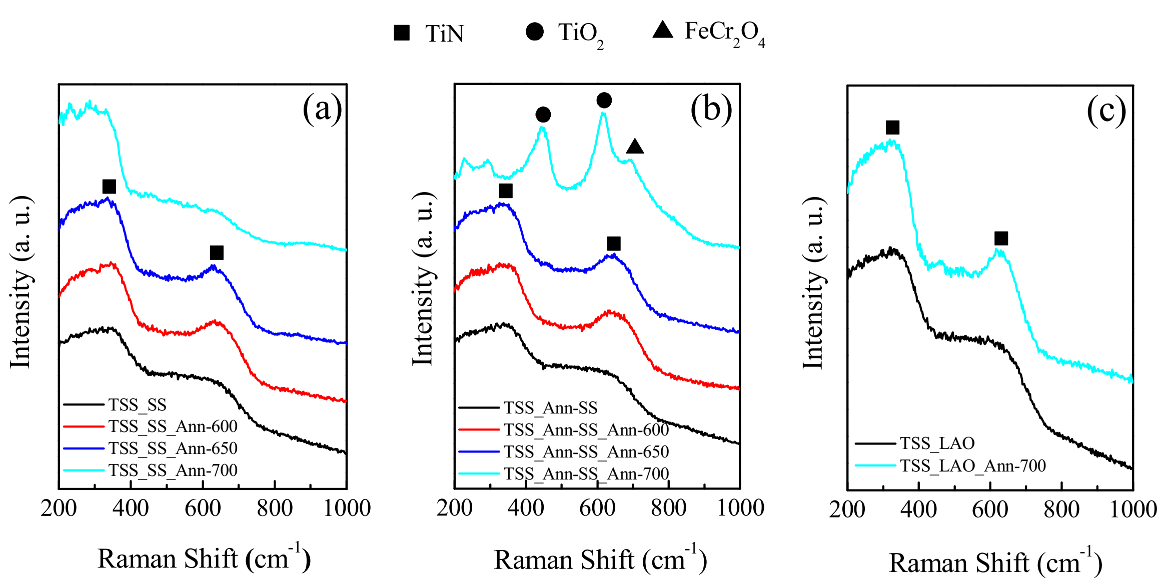

Fig. 6. Raman spectra of the pristine and the annealed spectrally-selective solar absorbers deposited on the mechanically polished stainless steel (SS) substrate (a), the annealed SS substrate (b), and the LAO substrate (c) at different annealing temperatures (black: pristine one; red: 600 °C; blue: 650 °C; cyan: 700 °C). The peaks marked with solid squares, solid circles, and solid triangles come from TiN, TiO_2, and $FeCr_2O_4$, respectively. (For interpretation of the references to color in this figure legend, the reader is referred to the web version of this article.).

ited on SS and annealed SS substrates demonstrate a high solar absorptance of ~92% even after annealing at 650 °C but lower absorbance of ~86% upon annealing at 700 °C due to decomposition and oxidation of TiN component in the cermets. However the degradation does not happen if the substrate is LAO. So a stable absorber up to 700 °C with a solar absorptance of ~94% is demonstrated.

Acknowledgments

This work is supported by "Solid State Solar-Thermal Energy Conversion Center (S^3TEC)", an Energy Frontier Research Center funded by the U.S. Department of Energy, Office of Science, and Office of Basic Energy Science under award number DE-SC0001299. J. B. acknowledges the support from the Robert A. Welch Foundation (E-1728), and F. C. thanks to the startup funding from Harbin Institute of Technology at Shenzhen.

Appendix A. Supporting information

Supplementary data associated with this article can be found in the online version at doi:10.1016/j.solmat.2016.10.012.

References

[1] D. Mills, Advances in solar thermal electricity technology, Sol. Energy 76 (2004) 19–31.
[2] D. Kraemer, B. Poudel, H.P. Feng, J.C. Caylor, B. Yu, X. Yan, Y. Ma, X.W. Wang, D.Z. Wang, A. Muto, K. McEnaney, M. Chiesa, Z.F. Ren, G. Chen, High-performance flat-panel solar thermoelectric generators with high thermal concentration, Nat. Mater. 10 (2011) 532–538.
[3] A. Lenert, D.M. Bierman, Y. Nam, W.R. Chan, I. Celanovic, M. Soljacic, E.N. Wang, A nanophotonic solar thermophotovoltaic device, Nat. Nanotechnol. 9 (2014) 126–130.
[4] F. Mauthner, W. Weiss, Solar Heat Worldwide, in: Markets and Contribution to the Energy Supply 2011, Solar Heating & Cooling Programme International Energy Agency, 2013.
[5] S. Meir, C. Stephanos, T.H. Geballe, J. Mannhart, Highly-efficient thermoelectronic conversion of solar energy and heat into electricpower, J. Renew. Sustain. Energy 5 (2013) 043127.
[6] L.A. Weinstein, J. Loomis, B. Bhatia, D.M. Bierman, E.N. Wang, G. Chen, Concentrating solar power, Chem. Rev. 115 (2015) 12797–12838.
[7] C.E.Kennedy, Review of mid to high temperature solar selective absorber materials, in: National Renewable Energy Laboratory, 2002.
[8] J. Moon, D. Lu, B. VanSaders, T.K. Kim, S.D. Kong, S. Jin, R. Chen, Z. Liu, High performance multi-scaled nanostructured spectrally selective coating for concentrating solar power, Nano Energy 8 (2014) 238–246.
[9] L. Tang, F. Cao, Y. Li, J. Bao, Z. Ren, High performance mid-temperature selective absorber based on titanium oxides cermet deposited by direct current reactive sputtering of a single titanium target, J. Appl Phys. 119 (2016) 045102.
[10] X. Yu, X. Wang, Q. Zhang, J. Li, J. Liu, Oxidation-resistant, solution-processed plasmonic Ni nanochain-SiO_x ($x < 2$) selective solar thermal absorbers, J. Appl Phys. 116 (2014) 073508.
[11] F. Cao, K. McEnaney, G. Chen, Z. Ren, A review of cermet-based spectrally selective solar absorber, Energy Environ. Sci. 7 (2014) 1615–1627.
[12] H.C. Barshilia, N. Selvakumar, K.S. Rajam, D.V.S. Rao, K. Muraleedharan, A. Biswas, TiAlN/TiAlON/Si_3N_4 tandem absorber for high temperature solar selective applications, Appl. Phys. Lett. 89 (2006).
[13] E. Céspedes, M. Wirz, J.A. Sánchez-García, L. Alvarez-Fraga, R. Escobar-Galindo, C. Prieto, Novel Mo–Si_3N_4 based selective coating for high temperature concentrating solar power applications, Sol. Energ. Mat. Sol. Cells 122 (2014) 217–225.
[14] F. Cao, D. Kraemer, L. Tang, Y. Li, A.P. Litvinchuk, J. Bao, G. Chen, Z. Ren, A high-performance spectrally-selective solar absorber based on a yttria-stabilized zirconia cermet with high-temperature stability, Energy Environ. Sci. 8 (2015) 3040–3048.
[15] F. Cao, D. Kraemer, T. Sun, Y. Lan, G. Chen, Z. Ren, Enhanced Thermal stability of W-Ni-Al_2O_3 cermet-based spectrally selective solar absorbers with tungsten infrared reflectors, Adv. Energy Mater. 5 (2015) 1401042.
[16] P.F. Li, B.A. Liu, Y.Z. Ni, K.K. Liew, J. Sze, S. Chen, S. Shen, Large-scale nanophotonic solar selective absorbers for high-efficiency solar thermal energy conversion, Adv. Mater. 27 (2015) 4585–4591.
[17] Z.Y. Nuru, C.J. Arendse, R. Nemutudi, O. Nemraoui, M. Maaza, Pt-Al_2O_3 nanocoatings for high temperature concentrated solar thermal power applications, Physica B 407 (2012) 1634–1637.
[18] H.G. Craighead, R.E. Howard, J.E. Sweeney, R.A. Buhrman, Graded-index Pt-Al_2O_3 composite solar absorbers, Appl. Phys. Lett. 39 (1981) 29–31.
[19] P. Patsalas, S. Logothetidis, Optical, electronic, and transport properties of nanocrystalline titanium nitride thin films, J. Appl. Phys. 90 (2001) 4725–4734.
[20] E. Valkonen, C.-G. Ribbing, J.-E. Sundgren, Optical constants of thin TiN films: thickness and preparationeffects, Appl. Opt. 25 (1986) 3624–3630.
[21] Y. Liu, Z. Wang, D. Lei, C. Wang, A new solar spectral selective absorbing coating of SS–(Fe_3O_4)/Mo/TiZrN/TiZrON/SiON for high temperature application, Sol. Energ. Mat. Sol. Cells 127 (2014) 143–146.
[22] S. Cheon, K.D. Kihm, Hg Kim, G. Lim, J.S. Park, J.S. Lee, How to reliably determine the complex refractive index (RI) of graphene by using two independent measurement constraints, Sci. Rep. 4 (2014) 6364.
[23] B. Johs, J.S. Hale, Dielectric function representation by B-splines, Phys. Status Solidi (a) 205 (2008) 715–719.
[24] H. Windischmann, Intrinsic stress in sputter-deposited thin-films, Crit. Rev. Solid State 17 (1992) 547–596.
[25] J. Cheng, C. Wang, W. Wang, X. Du, Y. Liu, Y. Xue, T. Wang, B. Chen, Improvement of thermal stability in the solar selective absorbing Mo–Al_2O_3 coating, Sol. Energ. Mat. Sol. Cells 109 (2013) 204–208.
[26] M. Bernard, A. Deneuville, O. Thomas, P. Gergaud, P. Sandstrom, J. Birch, Raman spectra of TiN/AlN superlattices, Thin Solid Films 380 (2000) 252–255.
[27] R. Chowdhury, R.D. Vispute, K. Jagannadham, J. Narayan, Characteristics of titanium nitride films grown by pulsed laser deposition, J. Mater. Res. 11 (1996) 1458–1469.
[28] V. Swamy, Size-dependent modifications of the first-order Raman spectra of nanostructured rutile TiO_2, Phys. Rev. B 77 (2008) 195414.
[29] X. Wu, M.-S. Zhang, Z. Yin, X. Ji, Q. Chen, Temperature characteristics of raman spectra in nanometer material titanium dioxide, Chin. Phys. Lett. 11 (1994) 685.
[30] A. Wang, K.E. Kuebler, B.L. Jolliff, L.A. Haskin, Raman spectroscopy of Fe-Ti-Cr-oxides, case study: martian meteorite EETA79001, Am. Mineral. 89 (2004) 665–680.